Since January 2020 Elsevier has created a COVID-19 resource centre with free information in English and Mandarin on the novel coronavirus COVID-19. The COVID-19 resource centre is hosted on Elsevier Connect, the company's public news and information website.

Journal of Molecular Liquids 318 (2020) 114082

Contents lists available at ScienceDirect

Journal of Molecular Liquids

journal homepage: www.elsevier.com/locate/molliq

Structural and physico-chemical evaluation of melatonin and its solution-state excited properties, with emphasis on its binding with novel coronavirus proteins

Nabil Al-Zaqri [a,b], T. Pooventhiran [c], Ali Alsalme [a], Ismail Warad [d], Athira M. John [e], Renjith Thomas [c,*]

[a] Department of Chemistry, College of Science, King Saud University, P.O. Box 2455, Riyadh 11451, Saudi Arabia
[b] Department of Chemistry, College of Science, Ibb University, P.O. Box 70270, Ibb, Yemen
[c] Department of Chemistry, St. Berchmans College (Autonomous), Changanassery, Kerala, India
[d] Department of Chemistry, Science College, An-Najah National University, P.O. Box 7, Nablus, Palestine
[e] Department of Chemistry, CHRIST (Deemed to be University), Bangalore, Karnataka, India

ARTICLE INFO

Article history:
Received 8 June 2020
Received in revised form 3 August 2020
Accepted 16 August 2020
Available online 23 August 2020

Keywords:
DFT
Melatonin
Coronavirus
NLO
NBO

ABSTRACT

Melatonin is a natural hormone from the pineal gland that regulates the sleep-wake cycle. We examined the structure and physico-chemical properties of melatonin using electronic structure methods and molecular-mechanics tools. Density functional theory (DFT) was used to optimise the ground-state geometry of the molecule from frontier molecular orbitals, which were analysed using the B3LYP functional. As its electrons interacted with electromagnetic radiation, electronic excitations between different energy levels were analysed in detail using time-dependent DFT with CAM-B3LYP orbitals. The results provide a wealth of information about melatonin's electronic properties, which will enable the prediction of its bioactivity. Molecular docking studies predict the biological activity of the molecules against the coronavirus2 protein. Excellent docking scores of −7.28, −7.20, and −7.06 kcal/mol indicate that melatonin can help to defend against the viral load in vulnerable populations. Hence it can be investigated as a candidate drug for the management of COVID.

1. Introduction

Melatonin is a sleep-regulating hormone created by the pineal gland and is released at night [1]. It has been found to have biological activity in almost all living organisms, including plants, animals, and microbes. It can quickly enter cells through the bilipid bilayer and exhibit scavenging activity towards oxygen free radicals as well as antioxidant properties due to its low molecular weight and amphiphilic nature [2].

Peripheral tissues have been found to show a high affinity towards this hormone (melatonin), and hence act on receptors and binding sites [3,4]. Studies reported by Tan et al. show that melatonin can also be produced in the mitochondria and hence tissue melatonin levels are more than that of serum levels, hence can be used as a molecule that targets mitochondria [5]. The main physico-chemical and biological properties of melatonin are sleep-inducing effects [6,7], antioxidant behavior [8–11], anti-inflammatory activity [10–13], antiapoptotic effects [14], and neuroprotective [8,9,15] effects. It also regulates various physiological functions of the brain. As melatonin can diffuse quickly through the blood-brain barrier, it is effectively used in the treatment of brain injuries [7,10,16]. Rapid eye-movement sleep-behavior disorder patients are managed by a combination treatment of melatonin and clonazepam [17–19]. The sensing of bacteria through Toll-like receptor-4, and regulation of bacteria through altered goblet cells and antimicrobial peptides, are all involved in the anticolitic effects of melatonin in inflammatory bowel disease [20]. Melatonin is involved in the aging process, growth towards puberty, and modulation of blood pressure [21]. This versatile compound blocks proangiogenic and antiangiogenic effects caused by docetaxel and vinorelbine, which are anti-tumor drugs, and it enhances their tumor-fighting behavior [22]. This molecule can modify the redox state of the rat pancreatic stellate cell.

Melatonin is an endogenous hormone that is involved in circadian rhythm control. It is inexpensive and safe as it has a significant effect as an antioxidant and anti-inflammatory. Melatonin, chemically *N*-acetyl-5-methoxytryptamine, is a tryptophan derivative, has multiple physiological effects, and can be used to treat many diseases related to virus infections, especially respiratory diseases. In COVID-19 patients with digestive complications, melatonin has positive effects [23].

* Corresponding author.
E-mail address: renjith@sbcollege.ac.in (R. Thomas).

https://doi.org/10.1016/j.molliq.2020.114082
0167-7322/

Melatonin can thus be used as an adjunctive or even as a regular therapy as no antiviral treatment is currently available. Electrochemical measurements of melatonin overflow demonstrate that melatonin secretion decreases with age [24]. Melatonin treatments result in the enhancement of essential oil production in *Salvia* species [25].

In the context of the recent COVID pandemic, melatonin can be researched as a potential molecule to control the dangerous effect of this disease. Rising patients' tolerance and decreasing the mortality in fatal virus infections would control the innate immune response and reduce inflammation during this period. Melatonin is a molecule with respective properties as it decreases the overreaction of the innate immune response and over-shoots inflammation, but also facilitates adaptive immune function [26].

Even though melatonin is a critical biomolecule, few works have been reported on the electronic structure and reactivity of this molecule except for a preliminary work reported by Turjanski and co-workers in 1999 using semi-empirical methods [27]. In this manuscript, we describe a detailed investigation into the quantum mechanical properties of melatonin, its spectral features, reactivity preferences, and the results of docking studies with three known structural protein receptors of the novel coronavirus-2. We found that melatonin docks strongly with the three proteins. We hypothesise that this compound can be used as an adjuvant medicine for the treatment of COVID-19. Also, significant rest by a person peacefully sleeping in dark surroundings will enhance the production of this hormone, which could help in the management of current patients or as a preventive measure in the vulnerable population.

2. Material and methods

The melatonin molecule was optimised using the Gaussian-09 [28] software package with the DFT-B3LYP functional and the 6-311G+ (2d, p) basis set. B3LYP is a commonly used functional and 6-311+(2d,p) basis set is medium-sized basis set with diffused functions over heavy atoms and polarization functions to bring accuracy. We performed frequency calculations to ensure that no imaginary frequency exists such that the geometry determined would correspond to a global minimum for reaching the optimised geometry. We used the same geometry for calculating frontier molecular analysis, natural bonding orbitals, and nonlinear optical studies. For UV–visible spectrum simulation, we used time-dependent density functional theory (TD-DFT) with long-range corrected CAM-B3LYP functionals with 6-311G+ (2d,p) as the basis set because electronic transitions are time-dependent phenomena. TD-DFT calculations are done using the optimised geometry obtained from B3LYP/6-311G+(2d,p) simulations. The frontier molecular orbitals were viewed from the checkpoint file generated during the optimisation calculations. A wavefunction file was generated during a single point ground state calculation job, using which the subsequent analysis performed. The melatonin molecule has more than two reaction sites, for example methoxy, carbonyl–amide, and purine ring. Reaction sites of melatonin calculated using the Multiwavefunction [29,30] software, for calculating total electrostatic potential [31], average localised ionization energies [31] and non-covalent interactions [31]. As it is reported that melatonin can be used as an adjuvant therapeutic material to fight COVID-19 [32], we decided to dock the molecule with three n-CoV-2019 protein's RCSB [33] site. Melatonin is effective in critical care patients by decreasing vessel permeability, anxiety, use of sedation, and increasing the quality of sleep, which may also be beneficial to COVID-19 patients for improved clinical outcome. Melatonin especially has a high health profile. Significant data indicate that melatonin reduces virus-related diseases and will possibly also be effective in patients with COVID-19. The target proteins were downloaded, cleaned, removed alien atoms and molecules and then used for docking. The energy received from the SwissDock software [34] and the score values received from PatchDock [35], as well as the docked results collected from Bio-discovery Studio software [36] are presented.

3. Results and discussion

3.1. Geometry of melatonin

The geometry of the molecule explains its rigid structure [37]. The structure of melatonin can be explained based on its physical parameters of bond lengths and bond angles between important atoms or groups, as shown in Fig. 1. The bond lengths of 1.3828, 1.3782 and 1.0076 Å are bonds of 1C-14N, 7C-14N, and 12H-14N, respectively, and the corresponding bond angles are109.0343°, 125.5437° and 125.4047° for 1C-14N-7C, 1C-14N-12H, and 7C-14N-12H, respectively. The bond angle of 117.8326° for 4C-25O-26C, having bond lengths of 1.3669 and 1.4227 Å for 4C—25O and 25O—26C, respectively. The bond lengths of 18C-21N, 21N-22H, 21N-23C, 23C—24O, and 23C—30C are 1.4564, 1.10147, 1.3716, 1.2284, and 1.5227 Å respectively, with the corresponding bond angles of 116.2826°, 127.4068°, 112.6290°, 121.1235°, 117.4685°, and 121.3891° for 18C-21C-22H, 18C-21C-23C, 22H-22N-23C, 21N-23C-24O, 21N-23C-30C, and 24O-23C-30C, respectively.

3.2. Frontier molecular orbital (FMO) properties of melatonin

The frontier molecular orbitals are highly reactive orbitals of other molecules, and some chemical descriptors [38] are shown in Table 1. The higher occupied molecular orbital (HOMO), lower unoccupied molecular orbital (LUMO), and energy gap of melatonin are −127.9554, −15.7755, and 112.1798 kcal/mol, respectively [39,40]. The energy gap is significant, indicating that the molecule is inherently stable. The ionization energy, electron affinity, hardness, softness, chemical potential, electronegativity, electrophilicity index, and nucleophilicity index of melatonin are 127.9554, 15.7755, 55.9989, 7031.7032, 71.8624, −71.8624, 46.1094, and 8539.8661 kcal/mol, respectively. Interaction of the melatonin with the biological target can be explained by the softness value. The softness value is high (7031.7032 kcal/mol), indicating that the molecule can positively interact with biological systems and show the desired effect [41].

3.3. Electron transition study and excited-state properties of melatonin in solution

The electron transition study explains electron-transfer excited states. We used the TD–DFT formalism using CAM-B3LYP functionals and 6-311G+ (2d,p) basis sets in an implicit solvation atmosphere of methanol using the IEFPCM model. As transmission occurs, some energy is also emitted. Melatonin electron transitions to HOMO having a pyrrole ring and oxygen (in methoxy), HOMO-1 over the pyrrole ring and ethyl carbons, and HOMO-2 over acetamide oxygen, nitrogen, and ethyl carbons with energies of −7.04, −7.23, and −8.79 eV, respectively. Melatonin electron transitions to LUMO which is over the pyrrole ring, LUMO+, which is over the pyrrole ring, oxygen (in methoxy), ethyl carbons, and acetamide nitrogen and carbon, and LUMO+2 having acetamide carbons, acetamide nitrogen, and carbons with energies of 0.37, 0.74, and 0.97 eV, respectively. The electronic spectral data using TD–DFT simulations indicate a significant λ_{max} of 256.07 nm in a methanol solvent. The transitions are due to the movement of electrons from HOMO-1 to LUMO (69%) and HOMO to LUMO (18%) with an oscillator strength of 0.1639. The electronic transitions are due to charge transfer transitions from one region of the molecule to another, which indicates its inherent stability due to electronic excitations.

3.4. Non-linear optical behavior of melatonin

Scientists and technologists working in the molecular electronics field are continuously searching for compounds with substantial non-linear optical (NLO) activity. Such compounds find immense application in electronic displays, surveillance equipment, and consumer electronic gadgets. Computationally, the ability of a molecule to act as an NLO material can be

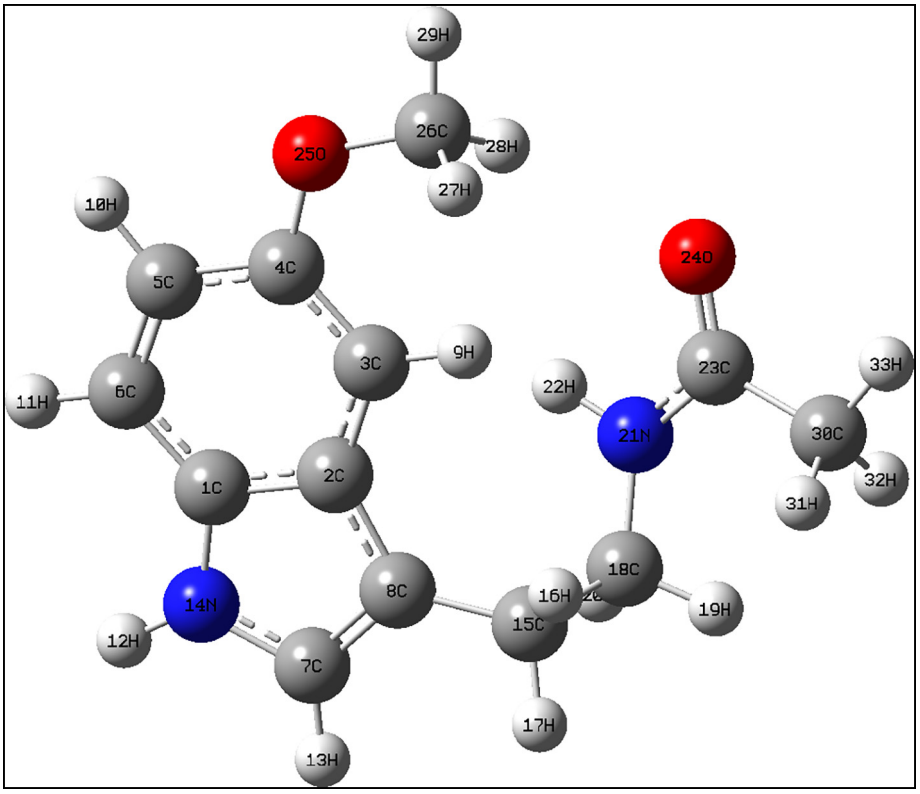

Fig. 1. Geometry of melatonin.

determined from the polarizability and hyperpolarizability data [42–45]. The NLO properties of melatonin are shown in Table 2. This is an essential behavior of melatonin that has a light absorption nature, movement of electrons or protons, as compared with a standard NLO material such as urea [46]. The dipole moment of melatonin is 4.4961 D, which is 1.4750 times greater than urea. Hyperpolarizability [47], mean polarizability, and anisotropy of the polarizability of melatonin are 544.5474, 180.1312, and 349.4465 esu, and which are 9.6495, 5.0524, and 5.0588 times greater than urea, respectively. The compound is not centrosymmetric, hence generates second-order spherical harmonics and beta hyperpolarizability functions. This compound can hence be used as an organic non-linear optically active substance in organic electronic appliances.

3.5. Nature of NBO study of melatonin

A molecule, especially one with profound biological activity, may have many intramolecular electron delocalisation and hyperconjugative stabilisation regions. Natural bond orbital analysis, which is a quantum mechanical method, is useful for this type of study. The molecular orbital properties of melatonin for the occupancy of the natural orbitals were performed by the NBO suite [43] embedded in the Gaussian software.

Table 1
Frontier molecular orbital properties for melatonin.

Chemical descriptors	Energy in kcal/mol
HOMO	−127.9554
LUMO	−15.7755
Ionization energy (I = εHOMO = −HOMO)	127.9554
Electron affinity (A = εLUMO = −LUMO)	15.7755
Energy gap = HOMO − LUMO	112.1798
Global hardness ($\eta = (I - A) / 2$)	55.9989
Global softness ($S = 1 / \eta$)	7031.7032
Chemical potential ($\mu = (I + A) / 2$)	71.8624
Electronegativity ($\chi = -\mu$)	−71.8624
Electrophilicity index ($\omega = \mu^2 / 2\eta$)	46.1094
Nucleophilicity index ($N = 1 / \omega$)	8539.8611

From donor-bonding orbital σ (C1-C2) with occupancy is 1.9578 to acceptor anti-bonding orbitals σ* (C3-C4), σ* (C5-C6), and σ* (C7-C8) exhibiting the transition, the energies are 17.15, 15.53, and 18.83 kcal/mol, respectively. From σ (C3-C4) with occupancy is 1.9684 to σ* (C5-C6), and the Rydberg orbital R* (C30) with the energies are 18.09 and 21.48 kcal/mol, respectively. From σ (C5-C6) having an occupancy is 1.9735 to σ* (C3-C4), R* (30), and R* (H33) with the energies are 18.04, 10.49, and 13.46 kcal/mol respectively, from σ (N21-C23) has occupancy 1.9915 to Rydberg orbital R* (C30) and R* (H33) with the energies are 11.05 and 30.53 kcal/mol, respectively, from σ (C23-O24) having the occupancy is 1.9932 to σ* (C1-C2), σ* (C2-C3), R* (C23) and R* (H33) with the energies are 41.93, 23.39, 78.00, and 193.98 kcal/mol, respectively, from σ (C23-C30) has occupancy is 1.9858 to R* (H17), R* (C18), R* (H19), R* (C23), R* (O24), R* (C30), R* (H33), σ* (C1-C2), σ* (C1-C6), σ* (C2-C3), σ* (C26-H27), σ* (C30-H31), σ* (C30-H32), and σ* (C30-H33) having the energies are 28.16, 21.27, 32.72, 87.90, 38.44, 425.33, 813.65, 497.63, 11.50, 136.64, 11.32, 41.85, 17.14, and 22.64 kcal/mol, respectively, from σ (O25-C26) having occupancy, is 1.9922 to R* (C30) and σ* (C1-C2) with the energies are 23.21 and 17.18 kcal/mol, respectively, from σ (C26-H27) to σ* (C1-C2) having the energy 12.48 kcal/mol with the occupancy is 1.9940, from σ (C30-H31) with the occupancy is 1.9763 to R* (H17), R* (C18), R* (H19), R* (C23), R* (O24), R* (C30), R* (H33), σ* (C1-C2), σ* (C2-C3), σ* (C23-O24), σ* (C30-H31), and σ* (C30-H32) having the energies are 19.45, 15.35, 21.77, 59.71, 25.54, 343.96, 489.68, 774.25, 102.18, 15.87, 27.07, and 24.50 kcal/mol respectively, from σ (C30-H32) with occupancy is 1.9781 to R* (H17), R* (C18), R* (H19), R* (C23), R* (O24), R* (C30), R* (H33), σ* (C1-C2), σ* (C2-C3), σ* (C30-H32), and σ* (C30-H33) having the energies are 17.26, 13.74, 21.60, 54.83, 20.96, 333.66, 470.61, 779.22, 99.22, 27.01, and 17.77 kcal/mol, respectively, and from σ (C30-H33) with the occupancy is 1.9877 to R* (H17), R* (C18), R* (C19), R* (C23), R* (C24), R* (O25), R* (C26), R* (H28), R* (C30), R* (H33), σ* (C1-C2), σ* (C1-C6), σ* (C2-C3), σ* (C2-C4), σ* (C18-H19), σ* (C23-O24), σ* (C26-H27), σ*

Table 2
Non-linear optics property for melatonin.

Non-linear property	Melatonin	Urea	Comparison of melatonin with urea
Dipole moment (μ)	4.4961 D	3.0482 D	1.4750 times greater than urea
Hyperpolarizability (β)	544.5474 esu	56.4324 esu	9.6495 times greater than urea
Mean polarizability (α_0)	180.1312 esu	35.6521 esu	5.0524 times greater than urea
Anisotropy of the polarizability (Δα)	349.4465 esu	69.0764 esu	5.0588 times greater than urea

(C30-C31), σ* (C30-H32), and σ* (C30-H33) having the energies are 53.21, 44.19, 62.43, 168.90, 69.68, 10.22, 20.79, 25.37, 1071.78, 1521.31, 28.56, 19.70, 311.41, 10.87, 10.40, 10.54, 24.34, 59.42, 64.53, and 31.23 kcal/mol, respectively.

From core bonding orbital C (C23), which has the occupancy 1.9994 electrons move to anti-bonding R* (C23), R* (C30), and R* (H33) with the transition energies are 111.01, 25.20, and 254.09 kcal/mol, respectively, from C (C23) with the occupancy is 19,994 to R* (H33), σ* (C2-C8), and σ* (C26-H28) having the energies are 165.30, 100.33, and 100.05 kcal/mol, respectively, from C (O24) to σ* (C26-H29) has the energy is 104.46 kcal/mol with occupancy is 1.9997, and from C (C30) having the occupancy is 1.9992 to R* (H17), R* (C23), R* (C30), R* (H33), σ* (C2-C8), σ* (C26-H28), σ* (C30-H31), and σ* (C30-H32) with the energies are 69.05, 1429.01, 485.11, 2218.86, 1038.03, 1094.80, 255.02, and 368.22 kcal/mol, respectively. From lone pair orbital n (N14) with the occupancy is 1.6360 to σ* (C7-C8) with the energy 34.96 kcal/mol, from n (N21) has the occupancy is 1.7134 to σ* (C23-O24) having the energy 48.68 kcal/mol, and from n (O24) having the occupancy is 1.9771 to R* (C23), R* (C30), R* (H33), σ* (C1-C2), and σ* (C2-C3) with the energies are 45.23, 251.23, 124.44, 180.36, and 80.00 kcal/mol, respectively. From anti-bonding orbital σ* (C1-C2) having the occupancy 0.4953 to R* (C30) and σ* (C2-C3) with the energies are 349.61 and 107.48 kcal/mol, respectively, from σ* (C5-C6) has occupancy is 0.3175 to R* (C30) with the energy is 108.84 kcal/mol, and from σ* (C23-O24) has occupancy is 0.2792 to R* (C30) with the energy is 78.70 kcal/mol. The inherent stabilisation of the molecule is evident from the series of hyperconjugative interactions presented above. These interactions can also be between the melatonin and the surrounding solvent molecules, which reveals its stabilisation in biological medium and also between the molecule and the target proteins used in the docking.

3.6. Total electrostatic potentials (ESP) and average localised ionization energy (ALIE) of melatonin

The electrostatic potential [48,49] explains how reactive sites can undergo nucleophilic or electrophilic addition or substitution reactions of melatonin, shown in Fig. 2 within 11.00 Bohr [3], and a color change from blue to red indicates charges on elements from −0.100 to 0.100. The blue color appears in both methoxy-oxygen and acetamide-oxygen; these are electron-rich sites, and electrophiles can quickly attack them. The red color appears on all of the hydrogens; these are electron-poor sites, and nucleophiles can quickly attack them.

The ALIE clarifies the stability of any molecule based on saturated and unsaturated bond electron movements which are localised or delocalised [48]. The number of the resonance structure is proportional to the stability of the molecule. The ALIE of melatonin shown in Fig. 3 is within the range of ±11.00 Bohr, color is from indigo to red, and the numerical value is from 0.000 to 2.000. The blue color of protons in the methoxy group, three protons in the six-membered ring in the indole group, methyl protons, and both adjacent carbons in the acetamide group are all sites that act as electrophiles. The red color of acetamide-carbon, conjugated carbon with oxygen atoms, and both acetamide-amide and methoxy groups are all sites that act as nucleophiles. These blue and red regions represent saturated bonds. The bluish-green regions are on indole rings to methoxy carbons via oxygen and acetamide chains. This indicates that delocalised electrons and unsaturated bonds lead to several resonance structures and explains the stability of melatonin. The electrophilic and nucleophilic reactive centres identified above interact with the COVID virus proteins and provide various electrostatic and non-covalent interactions and increases drug affinity.

3.7. Non-covalent interaction (NCI) properties of melatonin

Non-covalent interactions are a valuable biological property of molecules and are non-bonded directly, but are bound by some forces such as hydrogen bonding, van der Waals bonding, and/or steric constraints. Non-covalent interactions of melatonin are shown in Fig. 4 plotted as a graph with energy plotted versus a reduced density gradient [50]. Hydrogen bonds appear from −0.005 to −0.015 a.u. between oxygen and protons from the acetamide group. The Van der Waals force ranges

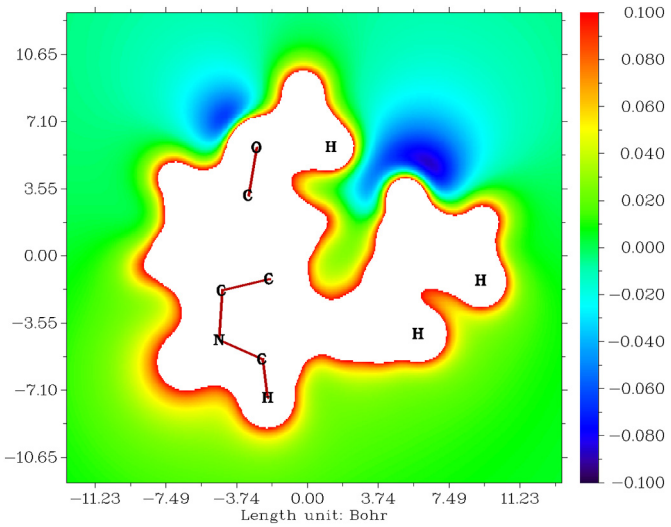

Fig. 2. Electrostatic potentials of melatonin.

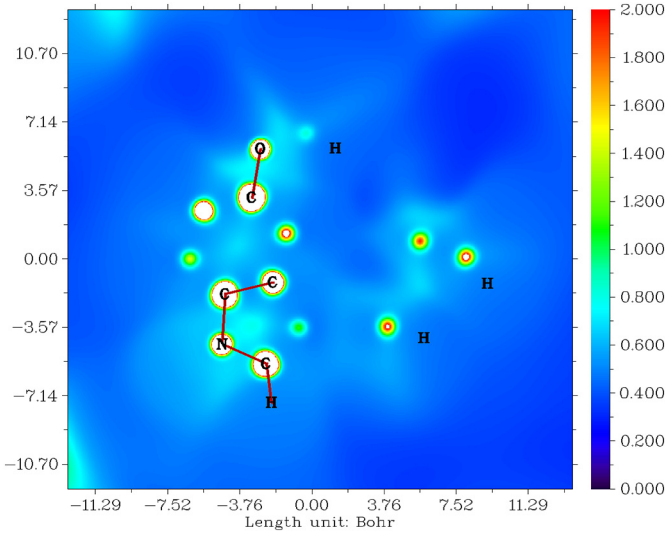

Fig. 3. Average localised ionization energy for melatonin.

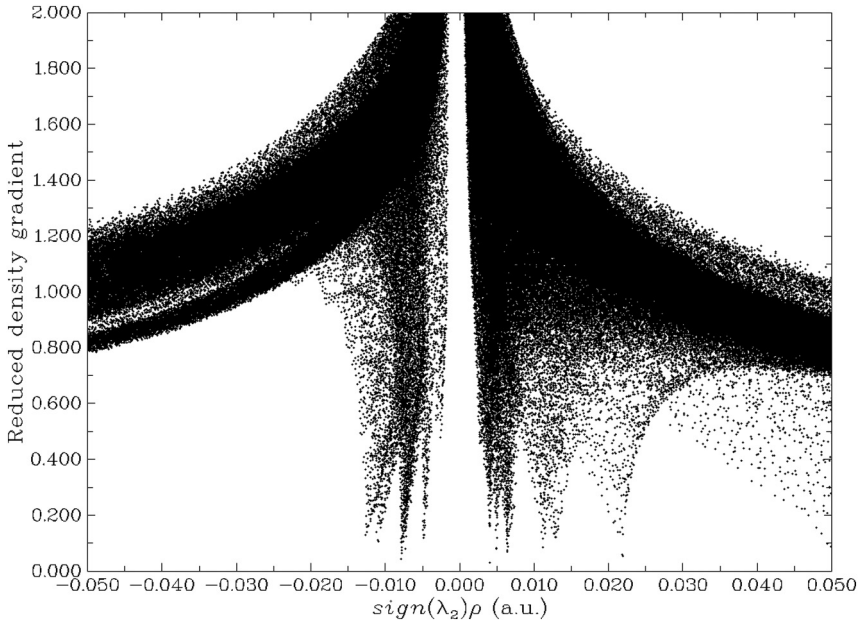

Fig. 4. Non-covalent interactions of melatonin.

from −0.005 to 0.004 a.u. between acetamide-oxygen and its adjacent protons in both methyl and methoxy groups. The steric force ranges from 0.004 to 0.023 a.u. between the indole ring, the methyl group, and the carbonyl-amide group. Non-covalent interactions are a group of interactions like hydrogen bond, pi-stacking, hydrophobic interactions, van der Waal's forces, ion-dipole interactions and dipole-dipole interactions responsible for the stabilisation of the molecule and the docking between melatonin and the COVID proteins.

3.8. Molecular docking

Molecular docking is one of the essential functions of biologically active molecules. This is the theoretical evidence to design the structure and reactivity relationship of a molecule. At present, the COVID-19 pandemic caused by a new strain of the coronavirus is creating havoc throughout the world. We made efforts to dock the melatonin with the three proteins isolated from the virus, represented through the PDB ID: 6LU7, 6M03, and 6W63 were deposited in the database as mentioned in the methodology section.

With the rapid spread of the novel coronavirus globally, the design of vaccines is of great importance. SARS-CoV-2 is an enveloped, non-segmented and single stranded, positive sense RNA virus. The best drug target among coronaviruses is the main protease, M^{pro}, also called 3CL protease [51,52]. This is a key coronavirus enzyme, and plays a vital role in mediating viral replication and transcription. It is identified as having a mechanism-based inhibitor [53,54].

The main targeting protease protein (PDB 6LU7) is widely studied. A series of frontier molecular orbital based interaction analyses were performed on the complex between the main protease of COVID-19 and the peptide-like inhibitor whose fundamental structure was obtained from the protein (PDB 6LU7) [55]. Another targeted protease protein, in an apo form (PDB 6M03), shows the most stable form after binding with the selected drug, Threonine 111 residue with the help of several covalent bond interaction with a −6 kcal/mol docking affinity [56]. Lasinavir, Brecanavir, Telinavir, Rotigaptide, 1,3-Bis-(2-ethoxycarbonylchromon-5-yloxy)-2-(lysyloxy)propane, and Pimelautide can be considered as the main protease inhibitors of COVID-19 by docking them to the binding cavities of apo (PDB 6M03) and holo (PDB 6LU7). Another protease protein (PDB 6W63) [57] is a reversible inhibitor. The flavonoid narcissoside is reported to have a high affinity towards the protease protein (PDB 6W63) according to molecular docking studies. Thus these three protease proteins (PDB 6LU7, PDB 6M03, and PDB 6W63) can be included in the category of non-structural proteins in the structure of SARS-CoV-2 [58,59].

From Table 3, the result from SwissDock explains the biological activity of melatonin with coronavirus proteins (PDB ID: 6LU7, 6M03, and 6W63). In general, the total ΔG is more than −5.00 kcal/mol is right active. Luckily melatonin has a total ΔG of −7.28, −7.20, and −7.06 kcal/mol with coronavirus2 proteins PDB ID: 6LU7, 6M03, and 6W63, respectively, and the total ΔG is directly proportional to the full fitness energy values which are −1219.44, −1194.87, and 1179.13 kcal/mol, respectively. It can also be seen from this table the: inter-full fitness, intra-full fitness, full solvent fitness, full surface fitness, ΔG complex polar solvent, ΔG complex nonpolar solvent, ΔG protein polar solvent, ΔG protein nonpolar solvent, ΔG ligand polar solvent, ΔG ligand nonpolar solvent, ΔG Van der Waals force, and ΔG electric force relationships between melatonin and coronavirus2 proteins, as referred.

The result from PatchDock are as follows: the score values are 3772, 3730, and 3588, total surface interacting area; 402.10, 416.60, and 427.80 Å [2]; and the minimum atomic contact energies are −150.61, −157.56, and −194.63 kcal/mol for melatonin with coronavirus2 proteins PDB ID: 6LU7, 6M03, and 6W63, respectively. Figs. 5 and S1 show the skeletal structure and protein residue interactions between melatonin and coronavirus2 protein PDB ID: 6LU7, 6M03, and 6W63. Table 4 explains what protein residues are interacting with melatonin, and details the residue names, labels, hydrophobic values, pKa values, average isotropic displacements, secondary structures, residue solvent accessibility, sidechain solvent accessibility, percent solvent accessibility, and percent sidechain solvent accessibility values of coronavirus2 proteins.

Table 3 and Fig. S2 show the residue structure of the favorable non-bond interactions between melatonin and coronavirus2 proteins. Table 5 lists favorable non-bond interactions of 6LU7 having conventional hydrogen bonds, carbon-hydrogen bonds, pi-donor hydrogen bonds, pi-sulfur, and pi-alkyl with melatonin. 6M03 has pi-sigma, pi-pi T-shaped, and pi-alkyl with melatonin, while 6W63 has pi-pi T-shaped, pi-alkyl, and pi-alkyl with melatonin along with the bond distance from chemistry. Fig. S2 and Table 6 show the residue structure

Table 3
SwissDock result for Melatonin with coronovirus2 proteins (PDB ID: 6LU7, 6M03 and 6W63).

	6LU7	6M03	6W63
Energy	−13.8144 kcal/mol	−12.942 kcal/mol	−13.0971 kcal/mol
Simple fitness	−13.8144 kcal/mol	−12.942 kcal/mol	−13.0971 kcal/mol
Full fitness	−1219.4406 kcal/mol	−1194.8722 kcal/mol	−1179.1298 kcal/mol
Inter full fitness	−39.8859 kcal/mol	−36.4921 kcal/mol	−35.9845 kcal/mol
Intra full fitness	2.02143 kcal/mol	2.2279 kcal/mol	3.07976 kcal/mol
Solvent full fitness	−1401.02 kcal/mol	−1380.43 kcal/mol	−1366.94 kcal/mol
Surface full fitness	219.444 kcal/mol	219.822 kcal/mol	220.715 kcal/mol
Extra full fitness	0 kcal/mol	0 kcal/mol	0 kcal/mol
ΔG complex solvent polar	−1401.02 kcal/mol	−1380.43 kcal/mol	−1366.94 kcal/mol
ΔG complex solvent nonpolar	219.444 kcal/mol	219.822 kcal/mol	220.715 kcal/mol
ΔG protein solvent polar	−1411.41 kcal/mol	−1385.67 kcal/mol	−1372.14 kcal/mol
ΔG protein solvent nonpolar	221.095 kcal/mol	221.3 kcal/mol	222.123 kcal/mol
ΔG ligand solvent polar	−9.24543 kcal/mol	−10.2561 kcal/mol	−11.0251 kcal/mol
ΔG ligand solvent nonpolar	5.98505 kcal/mol	6.02087 kcal/mol	5.53225 kcal/mol
ΔG van der Waals force	−39.8859 kcal/mol	−36.4921 kcal/mol	−35.9845 kcal/mol
ΔG electric force	0 kcal/mol	0 kcal/mol	0 kcal/mol
Total ΔG	−7.283887 kcal/mol 4	−7.2031846 kcal/mol	−7.057701 kcal/mol

of the unfavorable non-bond interactions between melatonin and coronavirus2 proteins. Protein 6LU7 does not have any unfavorable/steric interactions, protein 6M03 having three unfavorable non-bond interactions, and protein 6W63 having 33 unfavorable bump/non-bond interactions. Fig. S2 and Table 7 show unsatisfied bonds within melatonin interacting with coronavirus proteins. When interacting, protein 6LU7 has one hydrogen donor and one oxygen acceptor, protein 6M03 has two hydrogen donors and two oxygen acceptors, and protein 6W63 has one hydrogen donor and two oxygen acceptors with melatonin [60,61].

Table 8 shows non-covalent interactions between melatonin and coronavirus2 proteins. Hydrophobic groups of protein 6LU7 residues are A:His41, A:Leu141, A:Cys145, A:His164, A:Met165, and A:Glu166; those of protein 6M03 residues are A:His41, A:Met49, A:Phe140, A:Leu141, A:Cys145, A:Met165, A:Glu166, and A:Leu167; and those of protein residues 6W63 are A:His41, A:Cys44, A:Met49, A:Leu50, A:Met165, A:Glu166, A:Leu167, and A:Gln189 with melatonin as shown in Fig. S2 and Table 8. The hydrophilic groups of protein 6LU7 residues are A:His41, A:Asn142, A:His164, A:Glu166, A:His172, A:Asp187, A:Arg188, and A:Gln189; those of protein 6M03 residues are A:His41, A:Asn142, A:His163, A:His164, A:Glu166, A:His172, and A:Gln189; and those of protein 6W63 residues are A:His41, A:His164, A:Glu166, A:Asp187, A:Arg188, A:Gln189, and A:Gln192 with melatonin as shown in Fig. S3 and Table 8. Neutral groups of protein 6LU7 residues are A:Tyr54, A:Gly143, and A:Ser144; those of protein 6M03 residues are A:Gly143, A:Ser144, and A:Pro168; and those of protein 6W63 residues are A:Pro52, A:Tyr54, A:Arg188, and A:Thr190 with melatonin as shown in Fig. S4 and Table 8. Acidic groups of protein 6LU7 residues are A:Glu166 and A:Asp187; that of protein 6M03 residue is A:Glu166; and protein 6W63 residues are A:Glu166 and A:Asp187 with melatonin as shown in Table 8 and Fig. S5. Basic group interactions of protein 6LU7 residues are A:His41, A:His164, A:His172, and A:Arg188; those of protein 6M03 residues are A:His41, A:His163, A:His164, and A:His172; and those of protein 6W63 residues are A:His41, A:His164, and A:Arg188 as shown in Table 8 and Fig. S6. Tan et.al has shown that melatonin and derivatives has excellent biological responses like acting against oxidative stress and free radical scavenging [62–66]. Our studies show that melatonin molecule can interact with different proteins present in the n-CoV-19 virus and inhibit their proliferation. These results need further clinical follow up and could assist in the management of COVID pneumonia.

4. Conclusions

We conducted a detailed quantum-mechanical investigation of the hormone melatonin and regulation of the sleep-wake cycle. Natural bonding orbital studies revealed the intensity of several intramolecular interactions. The various frontier molecular orbital data explain the nature and physical parameters of melatonin, and the non-linear optical properties are compared with urea which is a standard material.

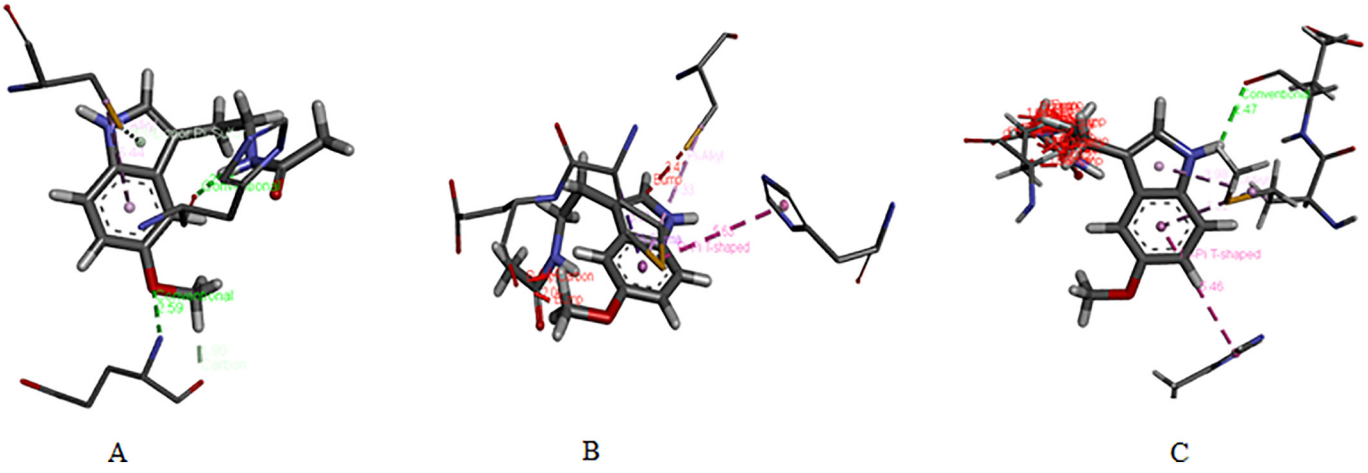

Fig. 5. Skeletal structure of interactions between melatonin and 6LU7 (A), 6M03 (B), and 6W63 (C) coronavirus2 protein residues.

Table 4
Interactions between melatonin and coronavirus2 protein residues.

PDB IDs	Name	Label	Hydrophobicity	pKa	Avg. isotropic displacement (Å)^2	Secondary structure	Residue solvent accessibility (Å)^2	Sidechain solvent accessibility (Å)^2	Percent solvent accessibility (Å)^2	Percent sidechain solvent accessibility (Å)^2
6LU7	Histidine	A:His41	−3.2	6	38.866	Helix	34.075	21.85	19.464	17.602
	Methionine	A:Met49	1.9	–	61.459	Turn	69.279	50.785	38.073	39.363
	Tyrosine	A:Tyr54	−1.3	10	37.275	Helix	177.112	58.584	80.665	34.767
	Leucine	A:Leu141	3.8	–	41.296	Coil	146.696	129.317	96.704	130.127
	Asparagine	A:Asn142	−3.5	–	45.276	Turn	167.056	128.991	113.179	133.44
	Glycine	A:Gly143	−0.4	–	38.475	Turn	60.921	15.095	85.049	62.827
	Serine	A:Ser144	−0.8	–	31.77	Coil	35.79	16.07	31.539	26.549
	Cysteine	A:Cys145	2.5	9	32.06	Turn	26.583	21.399	20.472	27.646
	Histidine	A:His164	−3.2	6	30.766	Sheet	57.755	46.916	32.991	37.796
	Methionine	A:Met165	1.9	–	37.842	Sheet	34.047	29.015	18.711	22.49
	Glutamic acid	A:Glu166	−3.5	4.3	36.048	Sheet	122.751	89.056	69.599	72.155
	Histidine	A:His172	−3.2	6	30.017	Sheet	116.35	52.725	66.461	42.475
	Aspartic acid	A:Asp187	−3.5	3.9	36.639	Coil	47.507	41.597	32.569	43.935
	Arginine	A:Arg188	−4.5	12	50.478	Coil	85.675	77.361	37.35	43.846
	Glutamine	A:Gln189	−3.5	–	43.289	Coil	134.002	110.464	75.154	88.119
6M03	Histidine	A:His41	−3.2	6	44.353	Helix	90.166	20.405	51.505	16.438
	Methionine	A:Met49	1.9	–	58.974	Helix	123.264	51.423	67.741	39.858
	Phenylalanine	A:Phe140	2.8	–	37.895	Coil	117.687	68.935	58.843	46.284
	Leucine	A:Leu141	3.8	–	44.94	Coil	122.991	116.737	81.078	117.47
	Asparagine	A:Asn142	−3.5	–	54.727	Turn	157.144	128.895	106.464	133.34
	Glycine	A:Gly143	−0.4	–	42.9	Turn	45.267	23.146	63.196	96.335
	Serine	A:Ser144	−0.8	–	36.803	Coil	21.118	6.917	18.61	11.427
	Cysteine	A:Cys145	2.5	9	38.353	Turn	31.983	26.799	24.631	34.622
	Histidine	A:His163	−3.2	6	33.44	Sheet	20.538	6.9	11.732	5.558
	Histidine	A:His164	−3.2	6	33.951	Sheet	61.269	57.028	34.998	45.942
	Methionine	A:Met165	1.9	–	57.177	Sheet	20.059	18.046	11.024	13.988
	Glutamic acid	A:Glu166	−3.5	4.3	50.616	Sheet	99.525	74.28	56.43	60.184
	Leucine	A:Leu167	3.8	–	52.523	Coil	45.031	40.757	29.685	41.013
	Proline	A:Pro168	−1.6	–	65.724	Turn	122.6	53.337	96.378	56.913
	Histidine	A:His172	−3.2	6	38.068	Sheet	77.66	41.72	44.361	33.609
	Glutamine	A:Gln189	−3.5	–	61.694	Coil	130.781	102.85	73.347	82.045
6W63	Histidine	A:His41	−3.2	6	24.23	Helix	109.161	50.29	62.354	40.513
	Cysteine	A:Cys44	2.5	9	45.568	Coil	60.751	12.814	46.786	16.554
	Methionine	A:Met49	1.9	–	66.152	Coil	82.928	78.088	45.574	60.526
	Leucine	A:Leu50	3.8	–	65.366	Coil	113.773	105.164	75.001	105.82
	Proline	A:Pro52	−1.6	–	45.346	Coil	39.512	5.032	31.061	5.369
	Tyrosine	A:Tyr54	−1.3	10	30.317	Helix	185.906	70.381	84.67	41.768
	Histidine	A:His164	−3.2	6	20.287	Sheet	125.035	91.897	71.422	74.032
	Methionine	A:Met165	1.9	–	32.264	Sheet	45.811	24.487	25.176	18.979
	Glutamic acid	A:Glu166	−3.5	4.3	28.999	Sheet	171.193	136.411	97.065	110.52
	Leucine	A:Leu167	3.8	–	34.562	Coil	66.89	48.305	44.095	48.608
	Proline	A:Pro168	−1.6	–	66.174	Turn	165.818	82.018	130.351	87.517
	Aspartic acid	A:Asp187	−3.5	3.9	23.642	Coil	45.934	39.584	31.491	41.809
	Arginine	A:Arg188	−4.5	12	45.901	Coil	103.831	91.196	45.265	51.687
	Glutamine	A:Gln189	−3.5	–	41.43	Coil	115.264	100.696	64.644	80.327
	Threonine	A:Thr190	−0.7	–	46.264	Coil	63.345	43.578	47.773	50.505
	Glutamine	A:Gln192	−3.5	–	40.842	Coil	75.091	18.832	42.114	15.023

Wavefunction studies gave information about electrostatic potentials, average localised ionization and non-covalent interactions. These data helped to predict the reactivity and identify the active site of the reactivity of the molecule. Melatonin docks with novel coronavirus proteins and shows a variety of interactions with an excellent docking score, which leads to inhibition of the virus proteins leading to its destruction. Hence, clinicians can consider incorporating melatonin also in the COVID-19 treatment regime after further studies.

Table 5
Favorable non-bond interactions between melatonin and coronavirus2 proteins.

PDB IDs	Distance (Å)	Category	Type	From	From chemistry	To	To chemistry
6LU7	2.59208	Hydrogen bond	Conventional hydrogen bond	A:GLU166:N	H-donor	:UNK0:O	H-acceptor
	2.90848	Hydrogen bond	Conventional hydrogen bond	:UNK0:H	H-donor	A:HIS164:O	H-acceptor
	1.89804	Hydrogen bond	Carbon hydrogen bond	:UNK0:H	H-donor	A:GLU166:O	H-acceptor
	4.14288	Hydrogen bond; other	Pi-donor hydrogen bond; Pi-sulfur	A:CYS145:SG	H-donor; sulfur	:UNK0	Pi-orbitals; Pi-orbitals
	5.43636	Hydrophobic	Pi-alkyl	:UNK0	Pi-orbitals	A:CYS145	Alkyl
6M03	3.92902	Hydrophobic	Pi-sigma	A:MET165:CA	C-H	:UNK0	Pi-orbitals
	5.63023	Hydrophobic	Pi-Pi T-shaped	A:HIS41	Pi-orbitals	:UNK0	Pi-orbitals
	5.32694	Hydrophobic	Pi-alkyl	:UNK0	Pi-orbitals	A:CYS145	Alkyl
6W63	2.47167	Hydrogen bond	Conventional hydrogen bond	:UNK0:H	H-donor	A:GLU166:O	H-acceptor
	5.46262	Hydrophobic	Pi-Pi T-shaped	A:HIS41	Pi-orbitals	:UNK0	Pi-orbitals
	4.3243	Hydrophobic	Pi-alkyl	:UNK0	Pi-orbitals	A:MET165	Alkyl
	3.98009	Hydrophobic	Pi-alkyl	:UNK0	Pi-orbitals	A:MET165	Alkyl

Table 6
Unfavorable non-bond between melatonin and coronavirus2 proteins.

PDB IDs	Distance (Å)	Category	Type	From	From chemistry	To	To chemistry
6LU7	Nil						
6M03	2.41199	Unfavorable	Unfavorable bump	A:CYS145:SG	Steric	:UNK0:C	Steric
	1.99847	Unfavorable	Unfavorable bump	A:GLU166:O	Steric	:UNK0:C	Steric
	1.63812	Unfavorable	Unfavorable bump; carbon hydrogen bond	:UNK0:H	Steric; H-donor	A:GLU166:O	Steric; H-acceptor
6W63	2.13058	Unfavorable	Unfavorable bump	A:GLN189:CA	Steric	:UNK0:C	Steric
	1.22635	Unfavorable	Unfavorable bump	A:GLN189:CA	Steric	:UNK0:H	Steric
	2.37385	Unfavorable	Unfavorable bump	A:GLN189:CB	Steric	:UNK0:C	Steric
	1.77146	Unfavorable	Unfavorable bump	A:GLN189:CG	Steric	:UNK0:C	Steric
	0.87813	Unfavorable	Unfavorable bump	A:GLN189:CG	Steric	:UNK0:H	Steric
	2.2544	Unfavorable	Unfavorable bump	A:GLN189:CG	Steric	:UNK0:N	Steric
	1.84974	Unfavorable	Unfavorable bump	A:GLN189:CG	Steric	:UNK0:H	Steric
	1.96838	Unfavorable	Unfavorable bump	A:GLN189:CD	Steric	:UNK0:C	Steric
	1.11711	Unfavorable	Unfavorable bump	A:GLN189:CD	Steric	:UNK0:C	Steric
	0.42714	Unfavorable	Unfavorable bump	A:GLN189:CD	Steric	:UNK0:H	Steric
	1.76113	Unfavorable	Unfavorable bump	A:GLN189:CD	Steric	:UNK0:H	Steric
	1.81942	Unfavorable	Unfavorable bump	A:GLN189:OE1	Steric	:UNK0:C	Steric
	0.89379	Unfavorable	Unfavorable bump	A:GLN189:OE1	Steric	:UNK0:H	Steric
	2.09198	Unfavorable	Unfavorable bump	A:GLN189:NE2	Steric	:UNK0:N	Steric
	1.10771	Unfavorable	Unfavorable bump	A:GLN189:NE2	Steric	:UNK0:C	Steric
	2.13841	Unfavorable	Unfavorable bump	A:GLN189:NE2	Steric	:UNK0:O	Steric
	0.54957	Unfavorable	Unfavorable bump	A:GLN189:NE2	Steric	:UNK0:C	Steric
	1.46472	Unfavorable	Unfavorable bump	A:GLN189:NE2	Steric	:UNK0:H	Steric
	1.1745	Unfavorable	Unfavorable bump	A:GLN189:NE2	Steric	:UNK0:H	Steric
	1.45993	Unfavorable	Unfavorable bump	A:GLN189:NE2	Steric	:UNK0:H	Steric
	1.25941	Unfavorable	Unfavorable bump	A:GLN189:HA	Steric	:UNK0:C	Steric
	0.61273	Unfavorable	Unfavorable bump	A:GLN189:HA	Steric	:UNK0:H	Steric
	1.52091	Unfavorable	Unfavorable bump	A:GLN189:HA	Steric	:UNK0:H	Steric
	1.40921	Unfavorable	Unfavorable bump	A:GLN189:HG1	Steric	:UNK0:H	Steric
	0.92704	Unfavorable	Unfavorable bump	A:GLN189:HG2	Steric	:UNK0:C	Steric
	0.19936	Unfavorable	Unfavorable bump	A:GLN189:HG2	Steric	:UNK0:H	Steric
	1.69586	Unfavorable	Unfavorable bump	A:GLN189:HE21	Steric	:UNK0:N	Steric
	1.11219	Unfavorable	Unfavorable bump	A:GLN189:HE21	Steric	:UNK0:C	Steric
	1.37181	Unfavorable	Unfavorable bump	A:GLN189:HE21	Steric	:UNK0:C	Steric
	1.39001	Unfavorable	Unfavorable bump	A:GLN189:HE21	Steric	:UNK0:H	Steric
	1.45408	Unfavorable	Unfavorable bump	A:GLN189:HE22	Steric	:UNK0:C	Steric
	0.8524	Unfavorable	Unfavorable bump	A:GLN189:HE22	Steric	:UNK0:C	Steric
	0.83783	Unfavorable	Unfavorable bump	A:GLN189:HE22	Steric	:UNK0:H	Steric

Table 7
Unsatisfied bonds in melatonin with coronavirus2 proteins.

PDB IDs	Name	Atom	Unsatisfied type
6LU7	:UNK0:H	H	Donor
	:UNK0:O	O	Acceptor
6M03	:UNK0:H	H	Donor
	:UNK0:H	H	Donor
	:UNK0:O	O	Acceptor
	:UNK0:O	O	Acceptor
6W63	:UNK0:H	H	Donor
	:UNK0:O	O	Acceptor
	:UNK0:O	O	Acceptor

CRediT authorship contribution statement

Nabil Al-Zaqri: Conceptualization, Funding acquisition. **T. Pooventhiran:** Investegation, Methodology, Original draft. **Ali Alsalme:** Investegation, Original draft. **Ismail Warad:** Resources, Review, Methods. **Athira M. John:** Methodology, Writing draft. **Renjith Thomas:** Conceptualization; Formal analysis; Investigation; Methodology; Project administration; Resources; Software; Supervision; Validation; Visualization; Writing - review & editing.

Declaration of competing interest

The authors declare that they have no known competing financial interests or personal relationships that could have appeared to influence the work reported in this paper.

Acknowledgements

Researchers Supporting Project number (RSP-2020/78), King Saud University, Riyadh, Saudi Arabia.

Appendix A. Supplementary data

Supplementary data to this article can be found online at https://doi.org/10.1016/j.molliq.2020.114082.

Table 8
Non-covalent interactions between melatonin and coronavirus2 proteins.

PDB IDs	Hydrophobicity	Hydrophilicity	Neutral group	Acidic group	Basic group
6LU7	A:His41, A:Leu141, A:Cys145, A:His164, A:Met165 and A:Glu166	A:His41, A:Asn142, A:His164, A:Glu166, A:His172, A:Asp187, A:Arg188 and A:Gln189	A:Tyr54, A:Gly143 and A:Ser144	A:Glu166 and A:Asp187	A:His41, A:His164, A:His172 and A:Arg188
6M03	A:His41, A:Met49, A:Phe140, A:Leu141, A:Cys145, A:Met165, A:Glu166 and A:Leu167	A:His41, A:Asn142, A:His163, A:His164, A:Glu166, A:His172 and A:Gln189	A:Gly143, A:Ser144 and A:Pro168	A:Glu166	A:His41, A:His163, A:His164 and A:His172
6W63	A:His41, A:Cys44, A:Met49, A:Leu50, A:Met165, A:Glu166, A:Leu167 and A:Gln189	A:His41, A:His164, A:Glu166, A:Asp187, A:Arg188, A:Gln189 and A:Gln192	A:Pro52, A:Tyr54, A:Arg188 and A:Thr190	A:Glu166 and A:Asp187	A:His41, A:His164 and A:Arg188

References

[1] J.H. Stehle, A. Saade, O. Rawashdeh, K. Ackermann, A. Jilg, T. Sebestény, E. Maronde, A survey of molecular details in the human pineal gland in the light of phylogeny, structure, function and chronobiological diseases, J. Pineal Res. 51 (2011) 17–43.

[2] R. Hardeland, S.R. Pandi-Perumal, Melatonin, a potent agent in antioxidative defense: actions as a natural food constituent, gastrointestinal factor, drug and prodrug, Nutr. Metab. 2 (2005) 22.

[3] D. Sugden, Melatonin: binding site characteristics and biochemical and cellular responses, Neurochem. Int. 24 (1994) 147–157.

[4] J. Vaněcek, A. Pavlík, H. Illnerová, Brain Res. 435 (1987) 359–362.

[5] D.-X. Tan, L.C. Manchester, L. Qin, R.J. Reiter, Melatonin: a mitochondrial targeting molecule involving mitochondrial protection and dynamics, Int. J. Mol. Sci. 17 (2016) 2124.

[6] K. Doghramji, J. Clin. Sleep Med. 3 (2007) S17–S23.

[7] W.T. Prater, M. Swamy, M.D. Beane, D.B. Lester, J. Behav. Brain Sci. 08 (2018) 117–125.

[8] M.A. Pappolla, Y.J. Chyan, B. Poeggeler, B. Frangione, G. Wilson, J. Ghiso, R.J. Reiter, J. Neural Transm. 107 (2000) 203–231.

[9] R. Sharma, C.R. McMillan, L.P. Niles, J. Pineal Res. 43 (2007) 245–254.

[10] R. Sharma, C.R. McMillan, C.C. Tenn, L.P. Niles, Brain Res. 1068 (2006) 230–236.

[11] K.M. Barlow, M.J. Esser, M. Veidt, R. Boyd, J. Neurotrauma 36 (2019) 523–537.

[12] A. Golabchi, B. Wu, X. Li, D.L. Carlisle, T.D.Y. Kozai, R.M. Friedlander, X.T. Cui, Biomaterials 180 (2018) 225–239.

[13] E. Esposito, S. Cuzzocrea, Curr. Neuropharmacol. 8 (2010) 228–242.

[14] S. Liu, C.O. Madu, Y. Lu, Oncomedicine 3 (2018) 37–47.

[15] D.X. Tan, Curr. Neuropharmacol. 8 (2010) 161.

[16] V. Srinivasan, S.R. Pandi-Perumal, G.J.M. Maestroni, A.I. Esquifino, R. Hardeland, D.P. Cardinali, Neurotox. Res. 7 (2005) 293–318.

[17] S.J. Mccarter, C.L. Boswell, E.K.S. Louis, G. Dueffert, N. Slocumb, B.F. Boeve, M.H. Silber, M.B.B. Ch, E.J. Olson, M. Tippmann-Peikert, NIH Public Access, Sleep Med. 14 (2014) 237–242.

[18] C. Jinny, F. Suzanne, C. Meaghan, W.C. Sean, J. Fi, C. Anderson, Differential impact of sleep deprivation and circadian timing on reflexive versus inhibitory control of attention, Sci. Rep. 10 (2020) 1–10.

[19] M.N.S. Gendy, D. Lagzdins, J. Schaman, B. Le Foll, Melatonin for Treatment-Seeking alcohol Use Disorder patients with sleeping problems: a randomised clinical pilot trial, Sci. Rep. 10 (2020) 1–10.

[20] S.W. Kim, S. Kim, M. Son, J.H. Cheon, Y.S. Park, Melatonin controls microbiota in colitis by goblet cell differentiation and antimicrobial peptide production through toll-like receptor 4 signalling, Sci. Rep. 10 (2020), 2232.

[21] H. Bagheri, A. Afkhami, P. Hashemi, M. Ghanei, RSC Adv. 5 (2015) 21659–21669.

[22] A. González-gonzález, A. González, N. Rueda, C. Alonso-gonzález, J.M. Menéndez, C. Martínez-campa, S. Mitola, S. Cos, Usefulness of melatonin as complementary to chemotherapeutic agents at different stages of the angiogenic process, Sci. Rep. 10 (2020), 4790.

[23] R.J. Reiter, Q. Ma, R. Sharma, Treatment of ebola and other infectious diseases: melatonin 'goes viral', Melatonin Res. 3 (1) (2020) 43–57.

[24] L.B. Diss, S.D. Robinson, Y. Wu, S. Fidalgo, M.S. Yeoman, B.A. Patel, Age-related changes in melatonin release in the murine distal colon, Chem. Neurosci. 4 (2013) 879–887.

[25] S.S. Bidabadi, J. Vanderweide, P. Sabbatini, Exogenous melatonin improves glutathione content, redox state and increases essential oil production in two Salvia species under drought stress, Sci. Rep. 10 (2020), 6883.

[26] D.X. Tan, R. Hardeland, Potential utility of melatonin in deadly infectious diseases related to the overreaction of innate immune response and destructive inflammation: focus on COVID-19, Melatonin Research 3 (1) (2020) 120–143, https://doi.org/10.32794/mr11250052 (Mar. 2020).

[27] A.G. Turjanski, R.E. Rosenstein, D.A. Estrin, Solvation and conformational properties of melatonin: a computational study, J. Mol. Model. 5 (1999) 271–280, https://doi.org/10.1007/s0089490050271.

[28] M. J. Frisch, G. W. Trucks, H. B. Schlegel, G. E. Scuseria, M. A. Robb, J. R. Cheeseman, G. Scalmani, V. Barone, B. Mennucci, G. A. Petersson, H. Nakatsuji, M. Caricato, X. Li, H. P. Hratchian, A. F. Izmaylov, J. Bloino, G. Zheng, J. L. Sonnenberg, M. Hada, … D. J. Fox, Gaussian09 Revision D.1 9.5 (n.d.).

[29] http://sobereva.com/multiwfn.

[30] T. Lu, F. Chen, Multiwfn: a multifunctional wavefunction analyser, J. Comp. Chem. 33 (2012) 580–592.

[31] E.R. Johnson, S. Keinan, P. Mori-Sánchez, J. Contreras-García, A.J. Cohen, W. Yang, Revealing noncovalent interactions, J. Am. Chem. Soc. 132 (2010) 6498–6506.

[32] R. Zhang, X. Wang, L. Ni, X. Di, B. Ma, S. Niu, C. Liu, R.J. Reiter, COVID-19: melatonin as a potential adjuvant treatment, Life Sci. 250 (2020), 117583, https://doi.org/10.1016/j.lfs.2020.117583.

[33] https://www.rcsb.org/.

[34] http://www.swissdock.ch/.

[35] https://bioinfo3d.cs.tau.ac.il/PatchDock/.

[36] A. Allouche, Software news and updates Gabedit—a graphical user interface for computational chemistry software, J. Comp. Chem. 32 (2012) 174–182, https://doi.org/10.1002/jcc.

[37] W.B. De Almeida, H.F.D. Santos, P.J. O'Malley, A molecular mechanics and semi-empirical conformational analysis of the herbicide diuron inhibitor of photosystem II, Struct. Chem. 6 (1995) 383–389.

[38] R.G. Parr, R.G. Pearson, Absolute hardness: companion parameter to absolute electronegativity, J. Am. Chem. Soc. 105 (1983) 7512–7516.

[39] R. Thomas, Y.S. Mary, K.S. Resmi, B. Narayana, B.K. Sarojini, G. Vijayakumar, C. Van Alsenoy, Two neoteric pyrazole compounds as potential anti-cancer agents: Synthesis, electronic structure, physico-chemical properties and docking analysis, J. Mol. Struct. 1181 (2019) 455–466.

[40] D.A. Thadathil, S. Varghese, K.B. Akshaya, R. Thomas, A. Varghese, An insight into photophysical investigation of (E)-2-fluoro-N′-(1-(4-nitrophenyl) ethylidene) benzohydrazide through solvatochromism approaches and computational studies, J. Fluoresc. 29 (2019) 1013–1027.

[41] K.E. Srikanth, A. Veeraiah, T. Pooventhiran, R. Thomas, K.A. Solomon, C.J.S. Soma Raju, J.N.L. Latha, Detailed molecular structure (XRD), conformational search, spectroscopic characterization (IR, Raman, UV, fluorescence), quantum mechanical properties and bioactivity prediction of a pyrrole analogue, Heliyon 6 (2020), e04106.

[42] Y.S. Mary, Y.S. Mary, R. Thomas, B. Narayana, S. Samshuddin, B.K. Sarojini, S. Armaković, S.J. Armaković, G.G. Pillai, Theoretical studies on the structure and various physico-chemical and biological properties of a terphenyl derivative with immense anti-protozoan activity, Aromat. Compd. (2019) 1–16, https://doi.org/10.1080/10406638.2019.1624974.

[43] K. Haruna, V.S. Kumar, Y.S. Sheena Mary, S.A. Popoola, R. Thomas, M.S. Roxy, A.A. Al-Saadi, Conformational profile, vibrational assignments, NLO properties and molecular docking of biologically active herbicide1,1-dimethyl-3-phenylurea, Heliyon 5 (2019), e01987, https://doi.org/10.1016/j.heliyon.2019.e01987.

[44] S. Beegum, Y.S. Mary, Y.S. Mary, R. Thomas, S. Armaković, S.J. Armaković, J. Zitko, M. Dolezal, C. Van Alsenoy, Exploring the detailed spectroscopic characteristics, chemical and biological activity of two cyanopyrazine-2-carboxamide derivatives using experimental and theoretical tools, Spectrochim. Acta A Mol. Biomol. Spectrosc. 224 (2020), 117414, https://doi.org/10.1016/j.saa.2019.117414.

[45] R. Thomas, Y.S. Mary, K.S. Resmi, B. Narayana, S.B.K. Sarojini, S. Armaković, S.J. Armaković, G. Vijayakumar, C.V. Alsenoy, B.J. Mohan, Synthesis and spectroscopic study of two new pyrazole derivatives with detailed computational evaluation of their reactivity and pharmaceutical potential, J. Mol. Struct. 1181 (2019) 599–612, https://doi.org/10.1016/j.molstruc.2019.01.014.

[46] Y.S. Priya, K.R. Rao, P.V. Chalapathi, A. Veeraiah, K.E. Srikanth, Y.S. Mary, R. Thomas, Intricate spectroscopic profiling, light harvesting studies and other quantum mechanical properties of 3-phenyl-5-isooxazolone using experimental and computational strategies, J. Mol. Struct. 1203 (2020), http://www.ncbi.nlm.nih.gov/pubmed/127461.

[47] E.D. Glendening, A.E. Reed, J.E. Carpenter, F. Weinhold, in: TCI, University of Wisconsin (Ed.), NBO Version 3.1, Madison, 1998.

[48] J.S. Al-Otaibi, A.H. Almuqrin, Y.S. Mary, R. Thomas, Modeling the conformational preference, spectroscopic properties, UV light harvesting efficiency, biological receptor inhibitory ability and other physico-chemical properties of five imidazole derivatives using quantum mechanical and molecular mechanics tools, J. Mol. Liq. 310 (2020), http://www.ncbi.nlm.nih.gov/pubmed/112871.

[49] F.A. Bulat, A. Toro-Labbé, T. Brinck, J.S. Murray, P. Politzer, Quantitative analysis of molecular surfaces: areas, volumes, electrostatic potentials and average local ionisation energies, J. Mol. Model. 16 (2010) 1679–1691.

[50] E.R. Johnson, S. Keinan, P. Mori-Sánchez, J. Contreras-García, A.J. Cohen, W. Yang, Revealing non-covalent interactions, J. Am. Chem. Soc. 132 (2010) 6498–6506.

[51] K. Anand, J. Ziebuhr, P. Wadhwani, J.R. Mesters, R. Hilgenfeld, Coronavirus main proteinase (3CLpro) structure: basis for design of anti-SARS drugs, Science (80-.). 300 (5626) (2003) 1763–1767.

[52] Z. Jin, et al., Structure of Mpro from SARS-CoV-2 and discovery of its inhibitors, Nature 582 (7811) (2020) 289–293.

[53] K.A. Peele, et al., Molecular docking and dynamic simulations for antiviral compounds against SARS-CoV-2: a computational study, Informatics Med. Unlocked 19 (May) (2020) 100345.

[54] R. Hatada, et al., Fragment molecular orbital based interaction analyses on COVID-19 main protease - inhibitor N3 complex (PDB ID:6LU7), J. Chem. Inf. Model. (2020) (in Press).

[55] Z. Zhang, B. Zhao, Y. Jin, Z. Liu, X. Yang, H. Rao, RCSB PDB - 6M03: the crystal structure of COVID-19 main protease in apo form, RCSB, https://www.rcsb.org/structure/6M03 2020. (Accessed 6 July 2020).

[56] S. Durdagi, B. Aksoydan, B. Dogan, K. Sahin, A. Shahraki, Screening of clinically approved and investigation drugs as potential inhibitors of COVID-19 main protease: a virtual drug repurposing study, ChemRxiv (March) (2020) 1–31 (A.D.).

[57] Mesecar, RCSB PDB - 6W63: Structure of COVID-19 Main Protease Bound to Potent Broad-spectrum Non-covalent Inhibitor X77, RCSB, 2020, https://doi.org/10.2210/pdb6W63/pdb.

[58] K. Dubey, R. Dubey, Computation screening of narcissoside a glycosyloxyflavone for potential novel coronavirus 2019 (COVID-19) inhibitor, Biom. J. 2019 (xxxx) (2020) 4–8.

[59] E.E.A. Osman, P.L. Toogood, N. Neamati, COVID-19: living through another pandemic, ACS Infect. Dis. (2020).

[60] J.S. Al-Otaibi, Y.S. Mary, Y.S. Mary, C.Y. Panicker, R. Thomas, Cocrystals of pyrazinamide with p-toluenesulfonic and ferulic acids: DFT investigations and molecular docking studies, J. Mol. Struct. 1175 (2019) 916–926.

[61] J.S. Al-Otaibi, Y.S. Mary, Y.S. Mary, R. Thomas, Quantum mechanical and photovoltaic studies on the cocrystals of hydrochlorothiazide with isonazid and malonamide, J. Mol. Struct. 1197 (2019) 719–726.

[62] D.X. Tan, L.C. Manchester, R.J. Reiter, W.B. Qi, M. Karbownik, J.R. Calvo, Significance of melatonin in antioxidative defense system: reactions and products, Biol. Signals Recept. 9 (2000) 137–159, https://doi.org/10.1159/000014635.
[63] D.X. Tan, L.D. Chen, B. Poeggeler, L.C. Manchester, R.J. Reiter, Melatonin: a potent, endogenous hydroxyl radical scavenger, Endocr. J. 1 (1993) 57–60.
[64] D.X. Tan, L.C. Manchester, L. Fuentes-Broto, S.D. Paredes, R.J. Reiter, Significance and application of melatonin in the regulation of brown adipose tissue metabolism: relation to human obesity, Obes. Rev. 12 (2011) 167–188, https://doi.org/10.1111/j.1467-789X.2010.00756.x.
[65] D.X. Tan, L.C. Manchester, R.J. Reiter, B.F. Plummer, Cyclic 3-hydroxymelatonin: a melatonin metabolite generated as a result of hydroxyl radical scavenging, Biol. Signals Recept. 8 (1999) 70–74, https://doi.org/10.1159/000014571.
[66] D.X. Tan, R. Hardeland, K. Back, L.C. Manchester, M.A. Alatorre-Jimenez, R.J. Reiter, On the significance of an alternate pathway of melatonin synthesis via 5-methoxytryptamine: comparisons across species, J. Pineal Res. 61 (2016) 27–40, https://doi.org/10.1111/jpi.12336.